



NEW PETROPHYSICAL MODEL FOR UNCONVENTIONAL HIGH-CO₂-CONTENT OIL RESERVOIRS

Jose Miguel Galindo¹, Jorge Arturo Camargo², Jose Wilder Losada², Jorge Ivan Chavarro², Freddy Humberto Escobar² and Carolina Charry¹

¹Ecopetrol, Gerencia de Operaciones de Desarrollo y Producción Putumayo

²Universidad Surcolombiana/CENIGAA, Avenida Pastrana - Cra 1, Neiva, Huila, Colombia

E-Mail: fescobar@usco.edu.co

ABSTRACT

It is known the existence of unquantified amount CO₂ produced from some fields in the Caguán Putumayo basin in Colombia. The effect of CO₂ on resistivity and porosity open hole logs have not been evaluated yet; then, it is proposed to build a new petrophysical interpretation model from available open hole logs in order to quantify the CO₂ concentration in the Caballos formation in the Caguán Putumayo basin to facilitate a better understanding of the thermodynamic behavior of the reservoir fluids. Knowing CO₂ significant subsurface concentration allows evaluating not only the impact in hydrocarbon reserves and production costs but also alternative management strategies for produced CO₂ to reduce environmental pollution. Reservoir CO₂ quantification resulted feasible by using porosity and neutron open hole logs superposition only if filtrate invasion is low or moderate. This method detects the residual CO₂ saturation; however, special drilling muds with null or low filtrate permits estimating virgin zone porosity. The method applies with no additional costs to all under saturated reservoirs containing CO₂ if density and neutron porosity logs are available. Neutron porosity can be replaced by NMR porosity.

Keywords: CO₂ saturation, porosity logs, NMR logs, depth of investigation.

INTRODUCTION

In the opinion of ecologists, CO₂ is the gas greenhouse gas causing warming global effect and represents a severe environmental problem, but, for experts, this resource can be no longer a problem and becomes an important energy source.

CO₂ flooding as an enhanced oil recovery technique was successfully started in 1972 in the Nelly-Snyder field in Texas. Currently, there exist more than some hundred active CO₂ injection projects in USA, Canada, Venezuela, Mexico, Trinidad, Libya and Turkey.

Due to the general concern on global warming, in the last decade, there have been undertaken several research projects related to CO₂ sequestration and injection CO₂ in depleted oil reservoirs or aquifer traps generally formed by sandstone. There are numerous references dealing with liquid CO₂ injection in brine-saturated cores to measure resistivity and acoustic velocity at high pressure and temperature conditions for simulating subsurface conditions. For instance, Onishi (2009) injected gas, liquid and supercritical CO₂ in brine-saturated cores at three different flow rates (0.5, 3 y 10 ml/min) and monitored the resistivity increase during injection. He calculated CO₂ saturation by applying Archie's equation knowing previously the formation resistivity factor (F), brine resistivity (R_w) and measuring true resistivity (R_t) for the reservoir rock-fluid set. Onishi (2009) concluded that the calculated water saturation agreed well with the amount of water displaced by CO₂ and the amount of CO₂ entering the reservoir rock can be accurately estimated by Archie's equation by measuring resistivity increase.

Nakatsuka (2010) presented a model for quantification CO₂ saturation injected in the sandstone core and utilized the resistivity index (IR) and the shale index (V_{sh}) measured by the gamma ray log.

Kim, Xue, Z. and Matsouka (2010) measured resistivity using an array of four electrodes along cores with injected CO₂ at supercritical state and concluded that seismic velocity and resistivity are useful for monitoring CO₂ by utilizing the fluid substitution theory and the resistivity index theory, respectively.

From the above experiences can be concluded that the CO₂ entrance in the reservoir rock increases significantly resistivity and decreases the acoustic velocity and, as a consequence CO₂ injection process can be monitored from Surface applying some categories of the electric method and/or seismic method by comparing measurement along the reference sections but with time lapse.

No information on petrophysical interpretation evaluating quantitatively the CO₂ effect on resistivity and porosity measurement during open well logging was found. Therefore, in this work, two core holder devices were built with the purpose of understanding the CO₂ effect on resistivity and sonic porosity in oil reservoirs. One device was used for measuring resistivity and the other one for acoustic velocity at reservoir conditions. The analysis of the measurement data allowed for the generating a new petrophysical model for correcting porosity and saturation due to high CO₂ content.



FIELD STUDY BACKGROUND

It is recognized that several oil fields in the Caguán Putumayo basin produce CO₂ in unmeasured amounts. However, it is believed that in the foothill, in the western sector of the same basin, a higher CO₂ content is produced. For this reason, a study focused on determining the CO₂ concentration in nine wells, five of which belonging to the western sector and four to the south of basin was conducted.

Franco *et al.* (2012) mentioned that there exists the highest CO₂ amount in the western area fields based upon the chromatography results given in CO₂ molar percentage: Caribe = 60.9%, Sucio = 60.9%, Quriyana = 93.6%, Churuyaco = 51.8%, San Antonio= 33.6% and Sucumbíos=72.8%. These results do not resolve the given problem since they do not permit the determination of the existing CO₂ amount in the different sandstones producing from the Caballos formation since the analyzed samples were collected from the production battery to which converges the production from different wells. The generalized stratigraphic column for the Caguán-Putumayo basin is given in Figure-1.

The Caballos formation is the main producing source from the basin. It consists of sandstone with interbedded shale and some thin carbon layers. The sandstone is formed primary by quartz grains; feldspar are less than 5% and other minerals in minimum amounts. The formation top is composed by gluconitic sandstone. Four different sandstone units can be differentiated in The Caballos formation. They are named from bottom to top: U1, U2, U3 and U4, Franco *et al.* (2012).

Table-1 presents reservoir and bubble point pressures for each one of the studied well; six wells belonging to the western area and 3 to the south. In all the cases, the reservoir is under under saturated conditions, then, by the time the well logs were run the reservoir rock contained only liquid hydrocarbon. On the other side, the production history reports very low GOR, compatible with under saturated fluids.

Table-1. Initial reservoir and bubble-point pressures for the studied well. After: Ecopetrol. Datos técnicos. Auditoria de reservas, año 2013.

| Well | PR (psi) | Pb (psi) |
|----------------|----------|----------|
| Sucumbíos 5 | 3300 | 1577 |
| San Antonio 14 | 3900 | 482 |
| Churuyaco 7 | 3900 | 1530 |
| Quriyana 1 | 3200 | 915 |
| Caribe 5 | 3037 | 1168 |
| Caribe 7 | 3037 | 1168 |
| Acaé 12 D | 4705 | 1600 |
| Acaé 6 | 4705 | 1600 |
| Loro 7A | 4705 | 1600 |

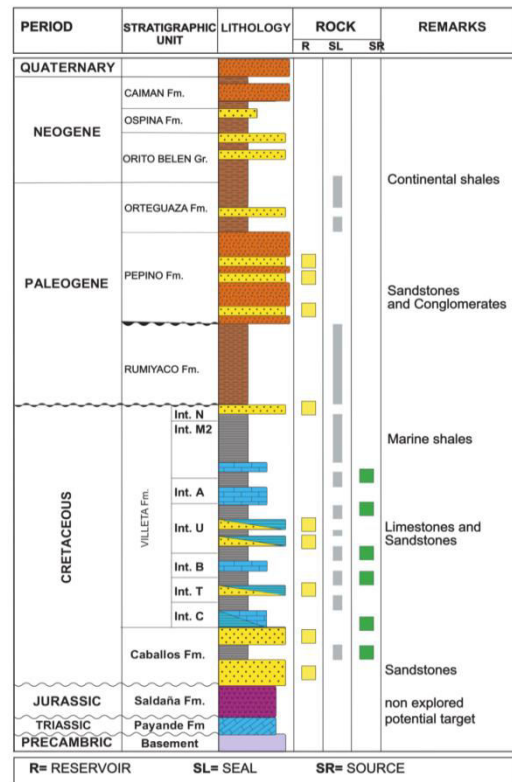


Figura-1. Generalized stratigraphic column for the Caguán-Putumayo basin. Taken from: Agencia Nacional de Hidrocarburos. Colombian Sedimentary Basins. Bogotá, 2007.

CO₂ EFFECT ON OPEN HOLE WELL LOG MEASUREMENTS

Conventional resistivity tools are devised for measuring rock-fluid resistivity at three levels: wash or flushed zone (R_{xo}), transition zone (R_i) and virgin zone (R_t) farther than the invaded zone by mud filtrate which reflects the true resistivity of rock and original fluids. The deep resistivity log (R_t) is very sensitive to the presence of such non-conductive fluids in the virgin zone as hydrocarbons; R_{xo} and R_i measure resistivities which resulted very influenced by the mud filtrate which displaces the original fluids. Like hydrocarbons, gas, liquid or supercritical CO₂ is a non-conductive substance; then, it is not possible to differentiate in the deep resistivity log (R_t) between hydrocarbon or CO₂ formations; moreover, the interpretation becomes harder in in oil reservoirs with high- CO₂ content.

Porosity logs

Measurements of sonic porosity, neutron, density magnetic resonance logs are subjected to the mud-filtrate invasion because their depth of investigation (DOI) is very low; then, their response is affected by the flushed and virgin zones. These tools respond differently depending upon lithology and gas or light fluids in the pore space. In high gas-contain reservoirs, porosity measured from



density logs is very high, while sonic porosity in well-compacted rocks has no influenced by gas, Hilchie (1962). However, there are small differences related to the tool design depending on the manufacturing company.

Density log

The density tool measures the density of electrons in the rock and a pore fluid which is related to total or bulk density of the rock-fluid set (ρ_b):

$$\rho_b = \phi \rho_f + (1 - \phi) \rho_{ma}$$

$$\rho_f = S_w \cdot \rho_w + S_o \cdot \rho_o + S_g \cdot \rho_g$$

If matrix density (ρ_{ma}) and fluid density (ρ_f) are known, then, the density tool allows estimating accurately the porosity.

$$\phi_D = \frac{\rho_{ma} - \rho_b}{\rho_{ma} - \rho_f}$$

When there exists residual oil in the flushed zone the total (ρ_b) from the density log is slightly affected since oil and water densities are fairly close. In such case, it is reasonable to assume $\rho_f=1$. in contrast, when residual hydrocarbon gas exists with density ranging from 0.1-0.3 g/cc, the resulting total density is very low; then, estimated porosity will be higher than the actual value. Customary, in gas zones the fluid density (ρ_f) is taken as the mud-filtrate density and it is accepted that the apparent porosity obtained from density tool is overestimated. In order to correct this effect, Hilchie (1982) suggested using a fluid density value of 0.7 g/cc in the above equation when gas density is unknown. It is deduced that residual oil having high CO₂ content has a density going from 0.6 to 0.9 g/cc at the Caballos formation depth. It produces an intermediate effect (between oil effect and hydrocarbon gas effect). Porosity from density log is slightly overestimated. Unfortunately in high-CO₂ -content oil reservoirs, it is not possible to estimate fluid density (ρ_f) because saturations and densities of oil and CO₂ are unknown; therefore, quantification of CO₂ is impossible from total (ρ_b) provided by the log.

Neutron log

The neutron log mainly responds to the amount of hydrogen atoms which are presented in the pore and fracture fluids (including clay water). This means that clean rocks with pores filled of liquid (water or oil), the apparent porosity from the neutron tool is a good indicator of total rock porosity whether or not pores are connected. The equation for the neutron log tool is:

$$\phi_N = \phi * IH_f + (1 - \phi) * IH_{ma} - \Delta \phi_{exc}$$

where IH is the hydrogen index which is found from:

$$IH_f = S_{xo} * IH_{mf} + S_o * IH_o + S_g * IH_g$$

The amount of hydrogen per formation unit volume is expressed by the hydrogen index (IH) which by definition is the unity for sweet water and less than one for hydrocarbon gases. This leads to clarify the existence of residual gas in the invaded zone causes less apparent porosity than the actual value. This minor hydrogen concentration is not corrected by the processing software of the neutron tool (Asquith and Krigowsky, 2007). Since CO₂ has no hydrogen in its structure, then, the neutron tool does not detect it. As a consequence, in oil reservoirs with CO₂ content, the hydrogen deficit is big and the apparent porosity is much less than the actual one.

Sonic log

It measures the transit time Δt used by a compressional wave to go throughout a foot of formation. Porosity is estimated by Willye equation, Bassiouni (1994):

$$\phi_s = \frac{\Delta t_c - \Delta t_{ma}}{\Delta t_{ma} - \Delta t_f}$$

$$\text{Where, } \Delta t_c = \phi \cdot \Delta t_f + (1 - \phi) \Delta t_{ma}$$

The fluid transient time is estimated by:

$$\Delta t_f = S_{xo} * \Delta t_{mf} + S_o * \Delta t_o + S_g * \Delta t_g$$

Since the investigation depth of the sonic tool is very low, it is assumed that the pore fluid is basically mud filtrate, then Δt_f is 189 or 185 $\mu\text{sec/ft}$, if dealt with sweet-water or salt-water based mud, respectively. The sonic tool responds well in clean rocks with intergranular uniform porosity. However, it only measures primary porosity. In theory, the transient time Δt_c is higher in reservoirs with high gas residual saturation and low invasion. Then, sonic porosity is higher than the actual value. The gas effect is corrected by multiplying by a factor of 0.7, Hilchie (1982). In practice, the sonic log only detects gas in unconsolidated rocks. It does not detect gas presence in compacted or consolidated rocks, like the Caballos formation.

NMR log

It is used only to study atomic nucleus having odd numbers of protons or neutrons as the case of a hydrogen atom ^1H , which behaves as a small magnet. The NMR tools are calibrated at the hydrogen magnetic resonance frequency. Analogous to the neutron tool, the NMR tool responds to the hydrogen amount or hydrogen index IH of the fluid in the pore space. It does not detect hydrogen in either rock matrix or clay minerals. The NMR equation (Hamada, 2008) is:

$$\phi_{NMR} = \phi * S_{gxo} * IH_g * P_g + \phi * IH_L * (1 - S_{gxo})$$

Assume a hydrogen index. $IH_L = 1$



$$\phi_{\text{NMR}} = \phi * [1 - S_{\text{gxo}} * (1 - I_{\text{H}_g} * P_g)]$$

Since CO₂ does not contain hydrogen, then, the NMR does not detect it. Therefore, apparent porosity from NMR logs in oil reservoirs with CO₂ is less than the actual value.

APPLICATION TO THE STUDIED FIELD

Gas detection is currently detected with the called “gas effect” using both neutron and density logs. The neutron tool was calibrated with sandstone matrix density (2.65 g/cc) in the nine studied wells and the porosity calculated from the density log used this density value. Oil has less density than water but about the same hydrogen index, but CO₂ –compared to water- has less density and its hydrogen index is zero. Therefore, oil rich in CO₂ has a less density than water and the hydrogen index is very low as the dissolved CO₂ content increases. When the density and neutron logs are superposed in compatible porosity scale of clean aquifers, they read equal porosity values. In oil reservoirs the neutron log reads a porosity value slightly lower than the density log. But, in gas reservoirs, the neutron reading is smaller than the density leading to a pattern known as “gas effect”. The two logs cross towards the high extreme value of the scale while the neutron goes towards the lower values. It is concluded for the studied field that if CO₂ is dissolved in oil crude, then density and neutron logs should display gas effect.

Notice that the neutron log reads all the hydrogen in the formation, including in clay minerals. This means that in reservoirs with clay the apparent porosity read by the tool is higher than the effective porosity and if gas exists, this can be undetected since they alter the sonic porosity in opposite directions. With the purpose of avoiding masking the existing CO₂ in oil reservoirs, there is a need of correcting density and neutron porosities due to clay content –convert them into effective porosities- before evaluating the magnitude of the gas effect by log superposition.

The combination of NMR and density logs responds for either gas presence or low density fluid similar to neutron-density crossover, this means that in front of a gas reservoir this superposition also shows gas effect. This combination allows to easily detect CO₂ presence since the NMR log has higher investigation depth than the neutron log and only detects hydrogen in the pore fluids and it is not sensitive to hydrogen in the clay minerals. It means that apparent porosity from NMR tool and the effective porosity are equal.

PROPOSED METHODOLOGY

The proposed method for CO₂ quantification uses neutron and density log superposition. Then, true porosity is estimated using any proposed equation for gas zones (DasGupta, Gaynard or Hilchie). This method applies to undersaturated reservoirs constituted by clean or clayey rocks in any formation (Caballos, Villeta and Pepino) if

neutron and density logs are provided and invasion zone is low. Neutron log can be replaced by NMR log which is only sensitive to fluids, eliminating the hydrogen effect in clay minerals which tends to mask the gas effect in the neutron log. This method detects either residual or minimum CO₂ saturation which was not displaced by the invaded fluid. The estimated saturation by this method would be the same to the virgin zone saturation in wells with special muds leading to low or zero.

Acoustic velocity measurement

Acoustic velocity throughout a fully saturated core was measured. First, a brine with 10000 ppm was used, second, brine concentration was increased to 30.000 ppm; then, the core was saturated with CO₂ and crude. In both cases, temperature ranged between 77 °F to 220 °F and pore pressure from 0 to 3000 psi, respectively. It was observed that acoustic velocities in crude and CO₂ decrease as the pressure increases. Also, temperature increment causes a reduction in acoustic velocity in crude and an increase of acoustic velocity CO₂.

Wan and Amos (1989) found that “velocity reduction of the compressive wave depends upon the pore pressure, temperature, porosity, among other factors. The pore pressure increment at constant confining pressure not only keeps pore and crack open and cancels the confining pressure effects but also increases CO₂ density; therefore, greater pore pressures cause a higher decrease in both P and S waves. In well consolidated sandstones, the increment of porosity tends to reduce CO₂ effect”.

Since the DOI of the Sonic tool is very low, measurements are mainly affected by wash zone fluids (mud filtrate and oil with dissolved CO₂). The fluid transit time for this case are represented by the following equation:

$$\Delta t_f = S_{x_o} * \Delta t_{mf} + S_o * \Delta t_o + S_{CO_2} * \Delta t_{CO_2}$$

At pressure and temperature conditions CO₂ and oil has net transit time 180 and 250 μsec/ft respectively. CO₂ transient time compared to the filtrate transient time in theory is 189 μsec/ft results to be very close so there is not enough contrast to determine CO₂ presence with the sonic log.

Resistivity measurements

Resistivity measurement in a 100% oil saturated core was infinite. Then, 25%, 50% and 75% of oil was successively displaced by CO₂ injection. In all cases resistivity was infinite. It was proved that CO₂, like oil, is a non-polar and non-conductive fluid. This experiment led to conclude that because of the lack in resistivity contrast of crude and CO₂, resistivity logs do not differentiate crude and CO₂ in the reservoirs, even, when CO₂ is dissolved in crude oil as for the case of the studied field.

**Table-2.** Petrophysical parameters for well Sucumbíos 5. Source: Ecopetrol-ICP.

| Depth (ft) | ∅ (%) | K (md) | Ro (Ω.m) | F (Ro/Rw) |
|------------|-------|--------|----------|-----------|
| 8869.83 | 6.9 | 1.8 | 89,11 | 171,27 |
| 8892.29 | 6.2 | 1.3 | 133,32 | 256,24 |
| 8894.50 | 5.8 | 3.8 | 141,15 | 271,28 |
| 8898.38 | 9.2 | 176 | 46,31 | 89,01 |
| 9050.50 | 10.8 | 152 | 36,01 | 69,21 |
| 9058.50 | 10.8 | 300 | 36,94 | 70,99 |
| 9079.08 | 8.4 | 270 | 56,72 | 109,02 |
| 9092.50 | 10.2 | 248 | 40,49 | 77,82 |
| 9101.42 | 10.0 | 72 | 44,76 | 86,03 |

Available information

Information of nine (out of 20) wells was used to build a model of petrophysical interpretation for quantifying CO₂ content. The remaining 11 wells had no complete information. The selected wells are: Sucumbíos 5, San Antonio 14, Quriyana 1, Churuyaco 7, Caribe 5, Caribe 7, Acaé 6, Acaé 12D, Loro 7A. A recent PLT log for well Sucumbíos 5 was also received along with a nuclear magnetic resonance log (MRIL) log (8784-9155 ft) and spectral gamma ray log of recovered cores from the caballos formation sandstone (8717-9107 ft) with their corresponding petrophysical analysis: porosity and permeability measurements, cementing coefficient of 1.93, saturation exponent of 1.79 and tortuosity coefficient of 1.

Since Caballos formation has very thick sandstones drilled with a 6-in diameter bit, only correction by invasion depth with tornado charts was applied. Neutron log was corrected by well diameter and temperature.

Water sampled from production battery was not used since water saturation depends exponentially on formation water resistivity (Rw). In all the wells chosen to build the petrophysical model the spontaneous potential (SP) has poor resolution possibly due to low filtrate-formation water resistivity contrast and high rock-fluid resistivity. This log was then not used for determining formation top, formation base and Rw. On the other hand, the gamma ray log shows an excellent definition. U1 sandstone has a growing-grain sequence from bottom to top. It is clean in the base and slightly clay in top. For its evaluation, it can be classified as clean sand.

Mud invasion and gas effects

The commercial package used for data processing corrects Rxo and Rt resistivities by invasion effects using special charts. It provides invasion diameter which was converted to invasion depth by:

$$DOI = \frac{Di - ID \text{ well}}{2}$$

Tabla-3. Invasion diameter for well Sucumbios 5.

| Depth (ft) | ID (in) | Rxo | Ri | Rt | Di (in) | DOI (in) | CO ₂ effect |
|------------|---------|-----|-----|-----|---------|----------|------------------------|
| 9013 | 6.28 | 6.0 | 692 | 605 | 20 | 7 | Yes |
| 9030 | 6.29 | 124 | 520 | 814 | 36 | 15 | No |
| 9060 | 6.22 | 61 | 165 | 458 | 55 | 24.5 | No |
| 9080 | 6.22 | 124 | 274 | 567 | 55 | 24.5 | No |

Table-4. Invasion diameter for well Caribe 7.

| Depth (ft) | ID (in) | Rxo | Ri | Rt | Di (in) | DOI (in) | CO ₂ Effect |
|------------|---------|-----|------|------|---------|----------|------------------------|
| 7808 | 5.88 | 130 | 915 | 1113 | 23 | 8.5 | Yes |
| 7830 | 5.88 | 257 | 458 | 458 | 18 | 6 | No |
| 7890 | 5.92 | 152 | 1368 | 2856 | 35 | 14.5 | No |
| 7920 | 5.92 | 143 | 303 | 303 | 18 | 6 | Si |



Rxo, Ri, Rt, and Di were read at different depths in front of sandstone U1. The DOI and the gas effect demonstration ratios for four wells are given in Table-3 through 7. In the first two wells; mud filtrate invasion was

deep enough that causes a significant reduction to gas effect. In the remaining two wells, with low invasion, the gas effect caused by CO₂ is evident.

Table-5. Invasion diameter for well San Antonio 14.

| Depth (ft) | ID (in) | Rxo | Ri | Rt | Di (in) | DOI (in) | CO ₂ Effect |
|------------|---------|-----|------|------|---------|----------|------------------------|
| 7808 | 5.88 | 130 | 915 | 1113 | 23 | 8.5 | Yes |
| 7830 | 5.88 | 257 | 458 | 458 | 18 | 6 | No |
| 7890 | 5.92 | 152 | 1368 | 2856 | 35 | 14.5 | No |
| 7920 | 5.92 | 143 | 303 | 303 | 18 | 6 | Si |

Table-6. Invasion diameter for well Acaé 6.

| Depth (ft) | ID (in) | Rxo | Ri | Rt | Di (in) | DOI (in) | CO ₂ Effect |
|------------|---------|-----|-----|-----|---------|----------|------------------------|
| 10544 | 10.45 | 437 | 343 | 353 | 20 | 5 | Yes |
| 10590 | 8.15 | 744 | 934 | 864 | 20 | 6 | Yes |
| 10620 | 8.33 | 409 | 471 | 451 | 20 | 6 | Yes |
| 10676 | 8.12 | 146 | 163 | 119 | 120 | 56 | Yes |
| 10720 | 8.20 | 54 | 53 | 43 | 120 | 56 | Yes |

As observed in Tables 3 through 6, in front of U1 sandstone, the DOI varies between 6" and 56"; intervals with DOI > 14" do not evidence gas effect (wells Sucumbíos 5 and Caribe 7). DOI < 12", low or moderate DOI's show gas effect.

Wiley and Patchett (1994) affirm that Invasion depths >18" reduce or eliminate the density and thermal neutron logs separation due to gas. The DOI difference is also reflected in the separation of virgin zone (Rt) and transition zone (Ri) resistivity logs. Wells Churuyaco 7 and Acaé 12D showing gas effect were included in the nine-well group for evaluating CO₂ content although do not possess the three resistivity logs.

"Gas Effect" interpretation in density and neutron logs

The observed gas effect is the result of CO₂ concentration in the pore space fluid and does not obey the hydrocarbon gas presence since undersaturated reservoirs do not have free hydrocarbon gas. In the gas effect zones, the density and neutron log separation varies between 4 and 9 porosity units. The gas effect is observed by a left

deviation of the density log while neutron log slightly -or nothing- deviates to the right. This pattern asymmetry due to gas effect suggests that porosity tools were affected at different levels by mud filtrate since DOI's are different.

In front of the CO₂ sandstones, the apparent porosities registered by the three logs after clayly correction are related in the following way:

$$\phi_D > \phi_N > \phi_S$$

Since sonic logs measure primary porosity and density and neutron tools measure total porosity including secondary porosity, so it is expected that sonic porosity to be the least. The following logs correspond to wells Sucumbíos 5, San Antonio 14, Caribe 7 and Acaé 6, in the zone corresponding to U1 basal sandstone of the Caballos formation which the most promising reservoir which constituted by quartzic clean sandstone with thick grain and porosities between 12-15 % and permeabilities between 200 and 300 md.

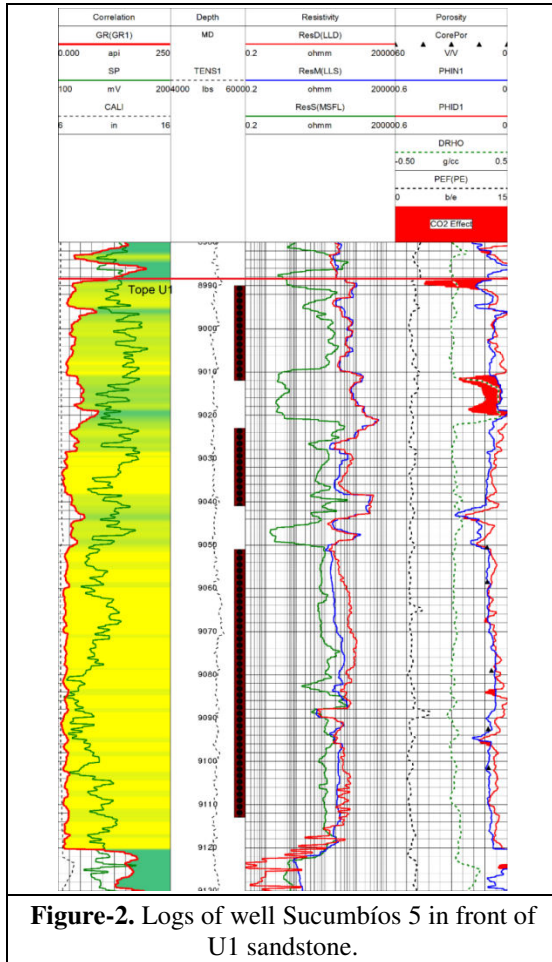


Figure-2. Logs of well Sucumbíos 5 in front of U1 sandstone.

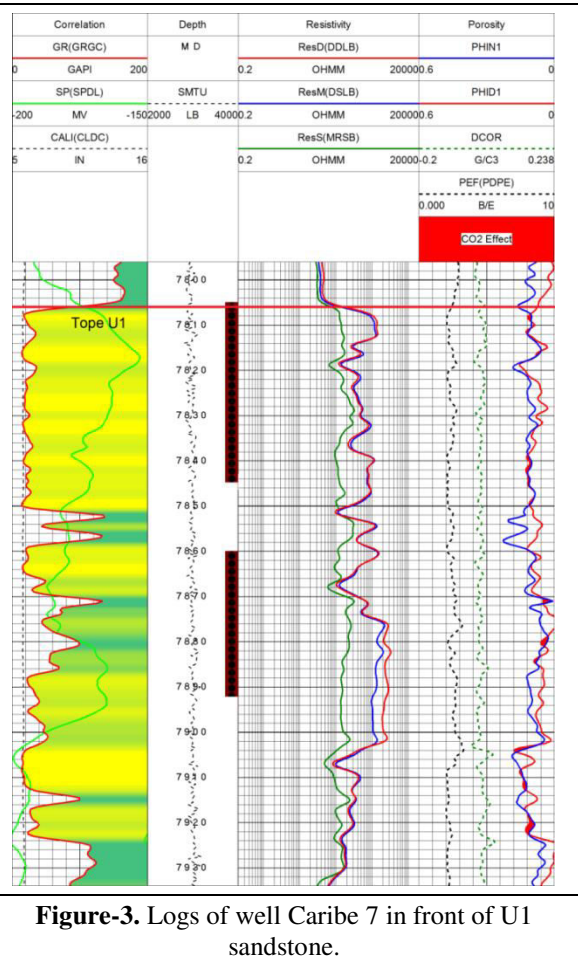


Figure-3. Logs of well Caribe 7 in front of U1 sandstone.

In well Caribe 7 the invasion was deep and eliminated almost the complete gas effect. In the 9010-9020ft interval a false gas effect is seen due to a bad contact of the density tool pad. In well San Antonio 14

invasion was deep and completely eliminated gas effect except in some specific zones. In well Acae-6 invasion was low and the CO₂ generated gas effect continuously, excepting the shale zones.

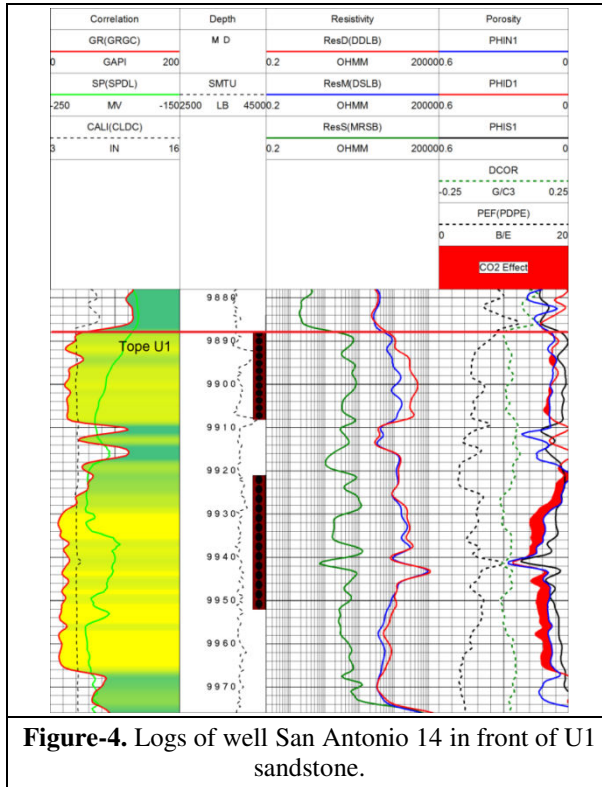


Figure-4. Logs of well San Antonio 14 in front of U1 sandstone.

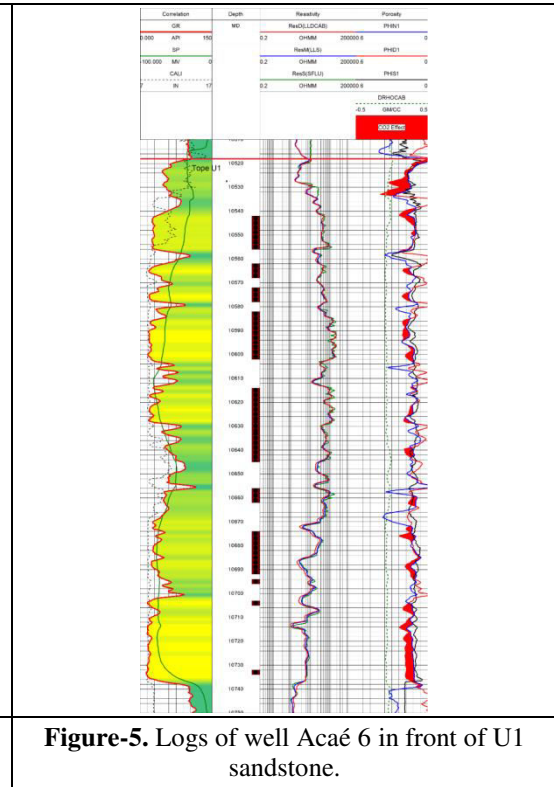


Figure-5. Logs of well Acaé 6 in front of U1 sandstone.

Clayly model

Clayly calculation was performed from the gamma ray log using Larionov method for ancient or consolidated rocks.

$$V_{sh} = 0.33 * (2^{2*I_{sh}} - 1)$$

Where,

$$I_{sh} = \frac{GR_{log} - GR_{min}}{GR_{max} - GR_{min}}$$

The estimated values matched well with DRX lab test son cores of well Sucumbíos 5. According to these results the clay volume is less than 10% and the most

abundant mineral is kaolinite. In lower amounts are found: chlorite, hilite and quartz powder, Franco *et al.* (2012) as illustrated in Figure-6.

Matrix density identification

The information taken from the well head logs indicates that the dominant matrix in Caballos formation corresponds to sandstone; then, a 2.65 g/cc density and 55,5 $\mu s/ft$ are used to estimate porosities. The photoelectric log (Pe) in front of the sandstone reads a value of 1.8 b/e that confirms that the reservoir rock is, in fact, a sandstone. In well Churuyaco 7 this log provided a higher value due to barite used in the drilling mud.

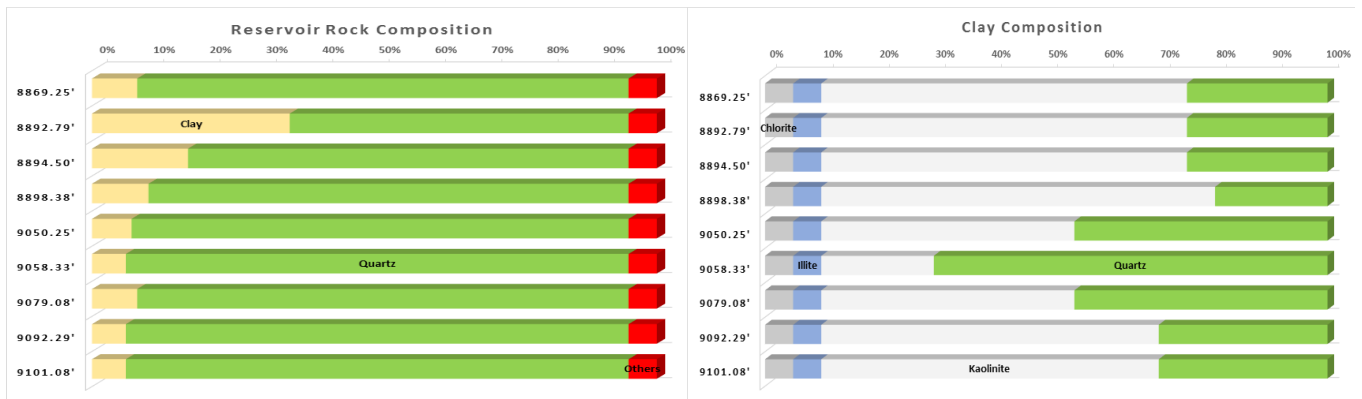


Figure-6. Matrix and clayly mineral composition of U1 Sandstone in well Sucumbíos 5. Taken from Franco *et al.* (2012).



Porosity model

Correction to neutron, density and sonic logs were applied by shale effect according to the following expressions proposed by Bassiouni (1994):

$$\begin{aligned} \phi'_N &= \phi_N - V_{shl} * \phi_{Nshl} \\ \phi'_D &= \phi_D - V_{shl} * \phi_{Dshl} \\ \phi'_S &= \phi_S - V_{shl} * \phi_{Sshl} \end{aligned}$$

Porosities from cores and well Sucumbíos 5 logs were compared as reported in Table-7. Values are fairly close. There is a need of determining true porosity from well logs since core information from other wells is unavailable. The true porosity (ϕ_T) in reservoir rocks saturated with gas or with a fluid of lower density than mud filtrate is conventionally estimated Gaymard equation.

$$\phi_T = \sqrt{\frac{\phi_N^2 + \phi_D^2}{2}}$$

However, other researchers, among them Ijasan (2013), state that porosities calculated from Gaymard equation especially in clean gas formations are very approximated and proposed different methodologies to estimate more accurate the true porosity from density and neutron logs. In this study, a direct and easy method proposed by Das Gupta (1997) to estimate true porosity,

$$\phi_T = \frac{2}{3}\phi_D + \frac{1}{3}\phi_N$$

Table-7. Porosities of Well Sucumbíos 5.

| Depth (ft) | ϕ_{Core} | ϕ_D (%) | ϕ_N (%) | ϕ_S (%) | ϕ_{NMR} (%) |
|------------|---------------|--------------|--------------|--------------|------------------|
| 9050.50 | 10.8 | 12.4 | 13.9 | 11.5 | 5.0 |
| 9058.50 | 10.8 | 9.0 | 9.73 | 7.2 | 10.5 |
| 9079.08 | 8.4 | 6.8 | 6.7 | 6.0 | 6.1 |
| 9092.50 | 10.2 | 4.0 | 8.2 | 9.6 | 7.0 |
| 9101.42 | 10.0 | 6.6 | 11.4 | 9.1 | 8.0 |

It is considered that this model provides better results under moderate invasion conditions since it takes into account that neutron and density tools are unequally affected by mud filtrate since DOI is different.

Water saturation model

Archie's equation was used for water saturation calculation using a = 1 m = 1.93, and n = 1.79 for all wells.

$$S_{WA} = \left(\frac{a}{\phi^m} * \frac{R_w}{R_t} \right)^{\frac{1}{n}}$$

Other water saturation models were considered since not all the Caballos formation sandstones are as clean as unit U1 and formation water salinity covers a wide range. Simandoux modified model produces good results in shaly sands saturated with salt water:

$$S_{WMS} = \left(\left(\frac{V_{sh}}{R_{sh}} \right)^2 + \frac{4\phi_e^m R_t}{aR_w * (1 - V_{sh})} - \frac{V_{sh}}{R_{sh}} \right)^{\frac{1}{2}} * \frac{aR_w * (1 - V_{sh})}{2\phi_e^m}$$

The Indonesia model produces good results in sands saturated with sweet water.

$$S_{WI} = \sqrt{\frac{1}{R_t}} * \frac{\sqrt{R_{sh}}}{(V_{sh})^{(1-0.5*V_{sh})}} + \sqrt{\frac{\phi_e^m}{aR_w}}$$

Table-8 shows saturation values for U1 sandstone obtained from Archie, Simandoux and Indonesia models.

It was concluded that water saturation by Archie's method is the most optimistic. Simandoux and Indonesia model estimate similar Sw values. Simandoux method was chosen for estimation of water saturation in the interpretation model.

Comparison of water saturation with production data

Tabla-9 allows comparing water saturation estimated from Simandoux method and water cut according to recent production history for each studied well. Sw for wells in Caribe field correlates well with water cut presented in the year 2013 production potential estimate. In the remaining wells the observed differences suggest that water saturation for those wells has increased during the well productive life.

**Table-8.** Sw summary calculated by each model.

| Well | Rw | Rt | SwA | SwMS | SwI |
|----------------|-------|---------|-------|-------|-------|
| Sucumbíos 5 | 0.134 | 374.06 | 16.60 | 19.54 | 19.73 |
| Quriyana 1 | 0.185 | 239.55 | 26.96 | 27.88 | 28.87 |
| Churuyaco 7 | 1.06 | 4551.87 | 11.33 | 15.13 | 15.39 |
| San Antonio 14 | 0.25 | 2700.83 | 7.26 | 9.34 | 9.43 |
| Caribe 5 | 1.55 | 3902.55 | 17.44 | 18.78 | 19.98 |
| Caribe 7 | 2.24 | 1310.39 | 40.93 | 40.17 | 42.70 |
| Acaé 12D | 0.133 | 205.95 | 24.92 | 28.71 | 28.80 |
| Acaé 6 | 0.12 | 539.36 | 13.35 | 13.41 | 14.88 |
| Loro 7A | 0.569 | 1034.39 | 30.28 | 27.04 | 30.80 |

Table-9. Saturation and water cut for the studied wells.

| Pozo | SwMS | % Water cut |
|----------------|-------|-------------|
| Sucumbíos 5 | 19.54 | 7.5 |
| Quriyana 1 | 27.88 | 60 |
| Churuyaco 7 | 15.13 | 60.7 |
| San Antonio 14 | 9.34 | 50 |
| Caribe 5 | 18.78 | 12 |
| Caribe 7 | 40.17 | 30 |
| Acaé 12D | 28.71 | - |
| Acaé 6 | 13.41 | 80 |
| Loro 7A | 27.04 | 73 |

Estimation of CO₂ saturation

If oil chemical composition shows high amounts of non-hydrocarbon components, there is a need of quantifying in the reserve estimation process to avoid overestimating hydrocarbon net volume. The existing CO₂ in the reservoirs under study lead to quantify the volumetric ratio between CO₂ and initial reservoir fluid. Two methods are proposed for the determination of CO₂ saturation from PVT analysis and open hole logs.

Method-1. From PVT analysis

This is more accurate for the determination of CO₂ Saturation. It was applied to Acaé 2, Quriyana 1 and

Sucumbíos 5 wells. It starts from the fluid composition obtained from PVT analysis, preferably from bottom sampling which are more representative than surface recombination. The methodology covers the following steps:

1) Find the total moles for an arbitrary reservoir fluid:

$$nt = \frac{P * Vt}{Z * R * T}$$

2) Obtain CO₂ moles from:

$$n_{CO_2} = Z_{CO_2} * nt$$

3) Find the equivalent mass of CO₂ moles:

$$m_{CO_2} = n_{CO_2} * MW_{CO_2}$$

4) Using the reservoir-condition density finds the volume occupied by the CO₂ mass:

$$V_{CO_2} = \frac{m_{CO_2}}{\rho_{CO_2}}$$

5) Find the volume fraction of CO₂ in crude oil from the following expression:

$$f_{CO_2} = \frac{V_{CO_2}}{V_t}$$

6) CO₂ saturation is calculated from:

$$S_{CO_2} = f_{CO_2} * (1 - Sw)$$

Z compressibility factor was provided by a phase-behavior simulator. CO₂ density was found with Ouyang (2011) correlation. Table-10 includes the CO₂ saturations calculated from PVT analysis.

Table-10. CO₂ Saturations.

| Well | CO ₂ (% mol) | CO ₂ (%Vol) | Sw (%) | S _{CO2} (%) |
|-------------|-------------------------|------------------------|--------|----------------------|
| Sucumbíos 5 | 47.25 | 19.64 | 18 | 16.10 |
| Quriyana 1 | 22.17 | 6.75 | 25 | 5.06 |
| Acaé 2 | 0.51 | 0.16 | 25 | 0.12 |



Method-2. From Porosity Logs Superposition

Considering in CO₂ rich reservoirs that neutron porosity decreases with respect to true porosity since the neutron tool ignores the CO₂ volume, then, the difference between true and neutron porosities correspond to the volume occupied by CO₂. NMR porosity can be utilized instead of neutron porosity,

$$\phi_{CO_2} = \phi_T - \phi_N$$

$$\phi_{CO_2} = \phi_T - \phi_{NMR}$$

CO₂ saturation is calculated by taking the porosity occupied by CO₂ divided by the rock true porosity estimated by Das Gupta method. Results for U1 sandstone are reported in Table-11.

$$S_{CO_2} = \frac{\phi_{CO_2}}{\phi_T} * 100$$

Table-11. Summary of true porosities and CO₂ saturations for U1 sandstone.

| WELL | | | True porosity | | | CO ₂ Saturation | | |
|----------------|--------------|--------------|---------------|--------------|--------------|----------------------------|----------------|----------------|
| | | | Dasgupta | Gaymard | Hilchie | Dasgupta | Gaymard | Hilchie |
| | ϕ_D (%) | ϕ_N (%) | ϕ_T (%) | ϕ_T (%) | ϕ_T (%) | S_{CO_2} (%) | S_{CO_2} (%) | S_{CO_2} (%) |
| Sucumbíos 5 * | 9.79 | 6.49 ** | 8.69 | 8.41 | 9.22 | 24.29 | 22.20 | 26.20 |
| Quriyana 1 | 10.70 | 8.70 | 10.04 | 9.76 | 10.01 | 13.34 | 10.91 | 12.54 |
| Churuyaco 7 * | 16.03 | 10.08 | 14.04 | 13.43 | 14.81 | 29.12 | 25.86 | 32.30 |
| San Antonio 14 | 13.57 | 9.22 | 12.12 | 11.62 | 12.39 | 22.26 | 19.15 | 23.80 |
| Caribe 5 | 10.73 | 8.22 | 9.89 | 9.58 | 10.01 | 17.85 | 15.17 | 15.85 |
| Caribe 7 | 12.81 | 10.97 | 12.20 | 11.93 | 12.10 | 10.29 | 8.26 | 7.20 |
| Acaé 12D | 14.49 | 5.83 | 11.60 | 11.10 | 13.47 | 50.54 | 48.21 | 57.05 |
| Acaé 6 | 17.91 | 11.86 | 15.90 | 15.21 | 18.33 | 25.62 | 22.29 | 34.71 |
| Loro 7A | 10.82 | 6.33 | 8.58 | 8.89 | 10.27 | 26.88 | 29.40 | 38.63 |

* CO₂ saturation decreased by Deep filtrate invasion

** NMR porosity.

As observed in Table-11, the higher CO₂ concentration is found in wells: Acaé 12D (50.54%), Loro 7A (26.88%) and Acaé 6 (25.62%). The least CO₂ concentration is found in wells: Caribe 7 (10.29%), Quriyana 1 (13.34%) and Caribe 5 (17.85%). It is known from well Sucumbíos 5 that CO₂ is high but the estimated concentration resulted decreased probably due to mud filtrate invasion.

CO₂ saturations found by this method for wells Sucumbíos 5 and Quriyana 1 resulted to be higher than 8% than CO₂ saturation found from PVT analysis. This difference may be due to PVT test reflects a local CO₂ saturation while saturations from logs separation correspond to an average of 7 porosity readings taken in each well at different depths in U1 sandstone.

In undersaturated reservoir with CO₂ contain, the logs separation method provide the minimum or residual saturation which was not displaced by mud filtrate. However, using special drilling mud with very low or zero invasion, this method could provide CO₂ in the virgin zone.

ADVANTAGES OF THE PROPOSED METHOD

CONCLUSIONS

1. CO₂ detection in reservoir is feasible by neutron and density logs superposition if mud invasion is low or moderate. This method detects the minimum or residual CO₂ saturation which was not displaced by mud filtrate. In special drilling muds with low or null invasion, the estimated saturation by this method should be equal to the saturation of virgin zone. This method applies to undersaturated reservoirs constituted by clean or clayey sandstones in any formation (Caballos, Villeta or Pepino) if neutron and density logs are available. Neutron log can be replaced by NMR log.

2. Although, the proposed method is approximated as are the log measurements, it is continuous and allows the evaluation of all the reservoirs in Caballos, Villeta and Pepino formations in any field of the basin.



Nomenclature

| | |
|-----------------------------|---------------------------------|
| a | Tortuositycoefficient |
| Di | Invasiondepth |
| DOI | Depth of investigation |
| ID | Internaldiameter |
| IR | Resistivityindex |
| I _{sh} | Shaleindex |
| F | Formation factor |
| GR _{min} | Minimum Gamma Ray |
| GR _{max} | MaximumGamma Ray |
| GR _{log} | InterestzoneGamma Ray |
| I _{H_L} | Fluid hydrogenindex |
| I _{H_{ma}} | Matrixhydrogenindex |
| I _{H_g} | Gas hydrogenindex |
| I _{H_{mf}} | Filtratehydrogenindex |
| m | Cementationexponent |
| n | Watersaturationexponent |
| P _b | Bubble-pointpressure |
| P _g | Gas pressure |
| PR | Reservorpressure |
| R _w | FormationwaterResistivity |
| R _{xo} | WhasedzoneResistivity |
| R _i | TransitionzoneResistivity |
| R _{sh} | Shaleresistivity |
| R _t | Virgen or true zone Resistivity |
| S | Saturation |
| S _{WA} | Watersaturationby Archie |
| S _{WMS} | WatersaturationbySimandoux |
| S _{WI} | Watersaturationby Indonesia |
| S _o | Oilsaturation |
| S _g | Gas saturation |
| S _{gxo} | Flushedzonesaturation |
| S _{CO2} | CO ₂ saturation |
| V _{sh} | Shalevolume |
| m | Cementationexponent |
| n | Watersaturationexponent |

Greek

| | |
|--------------------|-------------------------------------|
| ϕ | Porosity |
| ϕ_D | Densityporosity |
| ϕ_N | Neutronporosity |
| ϕ_N | Sonic porosity |
| ϕ_{NMR} | NMR porosity |
| $\Delta\phi_{exc}$ | Cave effectcorrection |
| Δt_{mf} | Filtratetransient time |
| Δt_{ma} | Matrixtransient time |
| Δt_o | Oiltransient time |
| Δt_g | Gas transient time |
| Δt_c | Compressional wave transient time |
| ϕ'_N | Neutron porosity corrected by shale |
| ϕ'_D | Density porosity corrected by shale |
| ϕ_T | True porosity |
| ρ_b | Total orbulkdensity |
| ρ_f | Fluid density |
| ρ_{ma} | Matrixdensity |

REFERENCES

- Asquith G. and Krygowski D. 2004. Basic well logs analysis. Tulsa: AAPG.
- Bassiouni Z. 1994. Theory, Measurement, and Interpretation of Well Logs (Vol. 7). United States of America: Society of Petroleum Engineers Inc.
- Dasgupta U. 1997. Houston Patente n° 5684299.
- Franco C. A., Bahamon Pedroza, J. I., Gonzalez Mosquera, J. G., Zapata Arango, J. F., Garcia, C. C., Henao, W. A., Madera K. 2012. January 1. Formation Damage Modeling Improves Well Candidate Selection and Stimulation Treatment Design in Western Area of Putumayo Basin, Colombia. Society of Petroleum Engineers. doi:10.2118/152400-MS.
- Hamada G. M. and Abushanab M. A. 2008. Better porosity estimate of gas sandstone reservoir using density and NMR logging data. Emirates Journal for Engineering Research. pp. 47-54.
- Hilchie D. W. 1982. Advanced well log interpretation. Golden, Colorado, United States of America. Indian Hill Books.
- Ijasaan O. and Torres C. 2013. Estimation of porosity and fluid constituents from neutron and density logs using an



www.arpnjournals.com

interactive matrix scale. SPWLA 54th Annual Logging Symposium (pp. 1-12). New Orleans: SPWLA.

Kim J. W., Xue Z. and Matsuoka T. 2010, January 1. Experimental Study On CO₂ Monitoring and Saturation With Combined P-wave Velocity and Resistivity. Society of Petroleum Engineers. doi:10.2118/130284-MS.

Nakatsuka Y., Xue Z., Yamada Y. and Matsuoka T. 2010. Experimental study on CO₂ monitoring and quantifying of stored CO₂ in saline formation using resistivity formation. International Journal of Greenhouse Gas Control. pp. 209-216.

Onishi K., Ishikawa Y., Yamada Y. and Matsuoka T. 2006. January 1. Measuring Electric Resistivity of Rock Specimens Injected With Gas, Liquid And Supercritical CO₂. Society of Exploration Geophysicists.

Ouyang L.B. 2011. New Correlations for Predicting the Density and Viscosity of Supercritical Carbon Dioxide Under Conditions Expected in Carbon Capture and Sequestration Operations. The Open Petroleum Engineering Journal, 14-15.

Wang Z. and Amos M. 1989. Effects of CO₂ flooding on wave velocities in rocks with hydrocarbons. SPE Reservoir Engineering. 429-436.

Wiley R. and Patchett J. G. 1994. The effects of invasion and density / thermal neutron porosity interpretation. SPWLA 35th Annual Logging Symposium. pp. 1-15.